Supporting Information

Manuscript title: A template-free and low temperature method for the synthesis of mesoporous magnesium phosphate with uniform pore structure and high surface area.

Authors: Jörn Hövelmann[1*], Tomasz M. Stawski[1], Rogier Besselink[1,2], Helen M. Freeman[1,3], Karen M. Dietmann[4], Sathish Mayanna[1], Brian R. Pauw[5] and Liane G. Benning[1,6,7]

Affiliations: [1]German Research Centre for Geosciences (GFZ), Interface Geochemistry, 14473 Potsdam, Germany; [2]Université Grenoble Alpes, CNRS, ISTerre, Grenoble 38000, France; [3]School of Chemical and Process Engineering, University of Leeds, Leeds LS2 9JT, UK; [4]GIR-QUESCAT, Department of Inorganic Chemistry, University of Salamanca, 37008 Salamanca, Spain; [5]Federal Institute for Materials Research and Testing (BAM), 12205 Berlin, Germany; [6]Department of Earth Sciences, Freie Universität Berlin, 12249 Berlin, Germany; [7]School of Earth and Environment, University of Leeds, Leeds LS2 9JT, UK.

***Corresponding author:** jhoevelm@gfz-potsdam.de

Journal: *Nanoscale*

Tables: 1

Figures: 7

No. of pages: 9

Table S1: Summary of struvite synthesis conditions, phases formed and struvite crystal morphologies

Synthesis ID	initial conditions		phases formed*	struvite crystal shape and size
	$c(Mg, P)_{mix}$ [mM]	pH		
S-1a	15	6.7	S	coffin-like; L: 10 – 30 µm, W: 5- 20 µm
S-1b	20	6.7	S	coffin-like; L: 10 – 30 µm, W: 5- 20 µm
S-1c	25	6.7	S	coffin-like; L: 10 – 30 µm, W: 5- 20 µm
S-2a	2	8.5	S	rod-like; L: 5 – 20 µm; W: 0.5 – 3 µm
S-2b	2.5	8.5	S	rod-like; L: 5 – 20 µm; W: 0.5 – 3 µm
S-2c	3	8.5	S	rod-like; L: 5 – 20 µm; W: 0.5 – 3 µm
S-3a	50	8	S	elongated, X-shaped; L: 50 - 200 µm; W: 20 – 100 µm
S-3b	250	8	S, N	rounded, anhedral; L/W: 50 – 100 µm
S-3c	500	8	S, N	rounded, anhedral; L/W: 10 – 20 µm
S-3d	1000	8	N, S, H	rounded, anhedral; L/W: 1 – 10 µm
S-4a	250	8.5	S, N	rounded, anhedral; L/W: 20 – 50 µm
S-4b	250	9	S, N	rounded, anhedral; L/W: 20 – 50 µm
S-4c	250	9.5	S	rounded, anhedral; L/W: 5 – 50 µm
S-4d	250	9.9	S	tabular, short-prismatic; L/W: 1 – 10 µm

**S = Struvite, N = Newberyite, H = Hannayite*

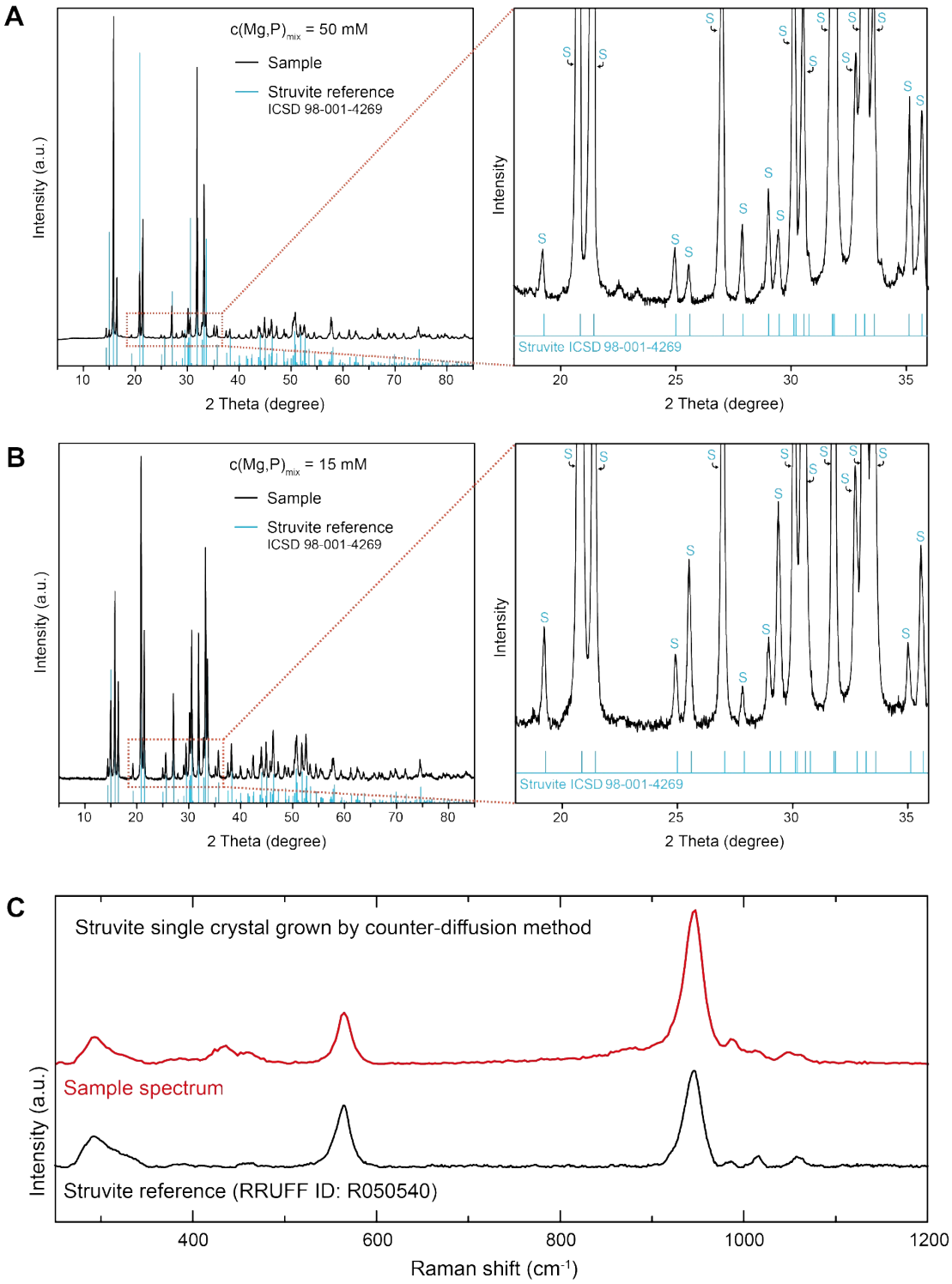

Fig. S1: (A) XRD pattern of struvite powder precipitated from mixed solutions with an initial concentration of c(Mg, P)mix = 50 mM. **(B)** XRD pattern of struvite powder precipitated from mixed solutions with an initial concentration of c(Mg, P)mix = 15 mM. A struvite reference pattern is shown in *blue* in A and B. **(C)** Representative Raman spectrum (*red*) of struvite single crystals grown by slow counter diffusion method. The struvite reference spectrum is shown in *black*.

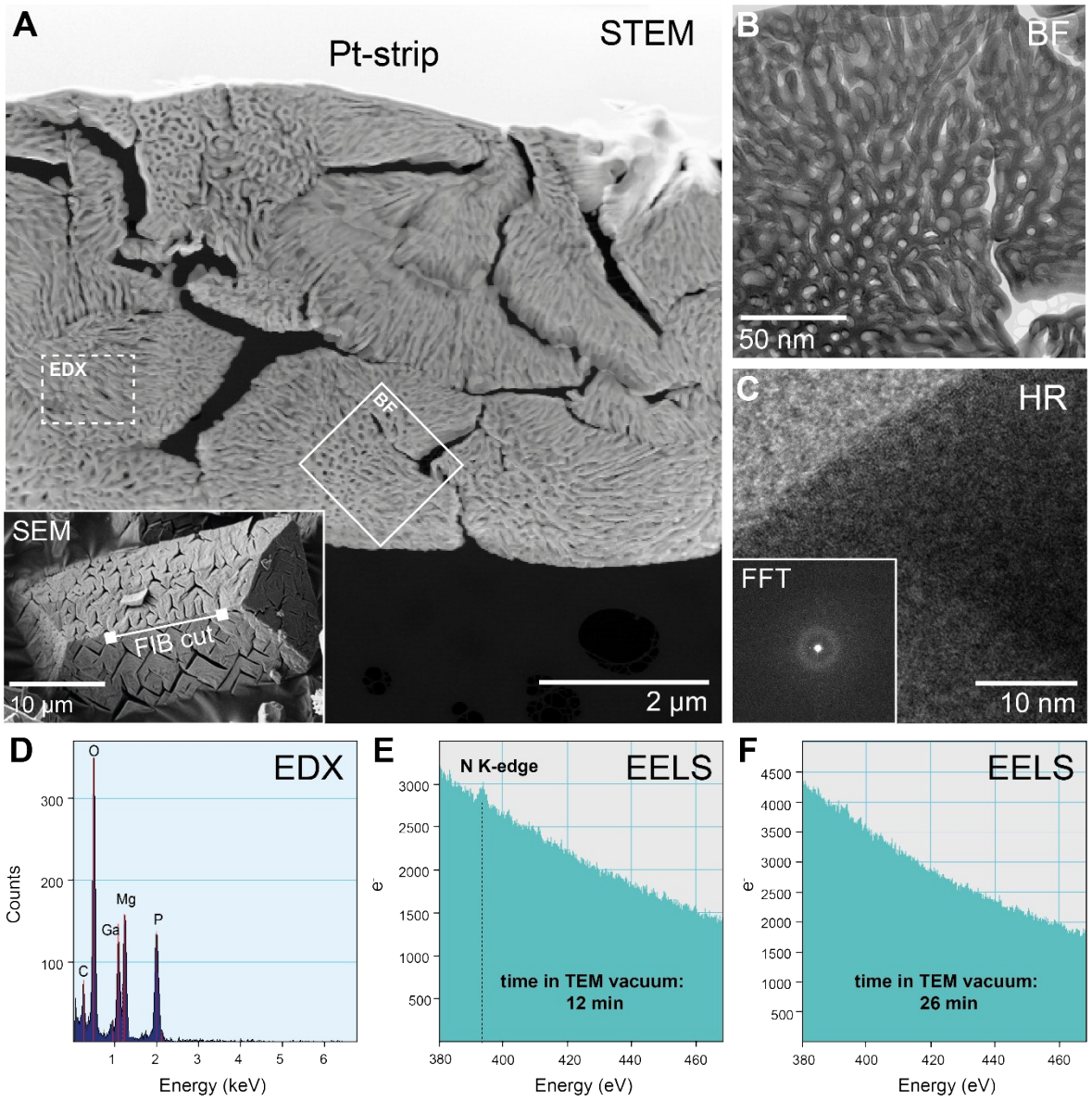

Fig. S2: FIB-TEM characterization of an as-synthesized struvite crystal. **(A)** Scanning Transmission Electron Microscopy (STEM) image of a FIB section prepared from the struvite crystal shown in the inset SEM image. The STEM image reveals lots of open cracks as well as a high internal porosity. **(B)** Bright Field (BF) TEM image of the area marked in A by a white square. **(C)** High Resolution (HR) TEM image and Fast Fourier Transform (FFT; inset) showing the amorphous nature of the material. **(D)** EDX analysis of the area marked by a dotted rectangle in A showing the presence of Mg and P. The Ga-peak originates from Ga-ion bombardment during preparation of the FIB section, whereas the C-peak comes from the C-coating that was applied to the crystal for SEM imaging preparation. **(E, F)** Electron Energy Loss Spectra (EELS) showing the decay of the N K-edge during TEM investigations. The spectrum in E, taken after ca. 12 min in TEM vacuum, shows only a weak N K-edge. This edge is completely absent in F (taken after 26 min) indicating a continuous loss of N in the high vacuum of the TEM.

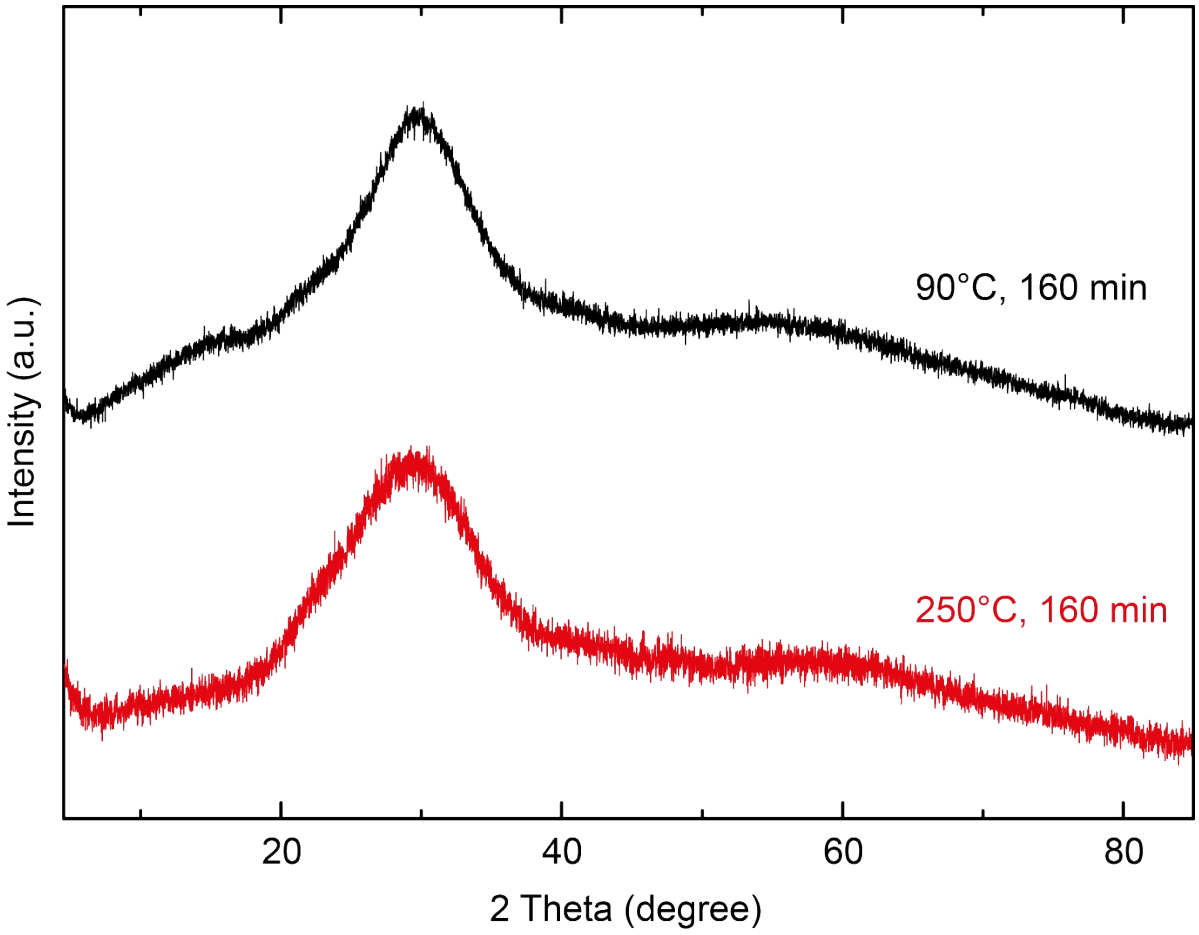

Fig. S3: XRD patterns of struvite powders thermally treated for 160 min at 90°C (black) and 250°C (red) indicating complete absence of long-range order (i.e., crystallinity) in the samples.

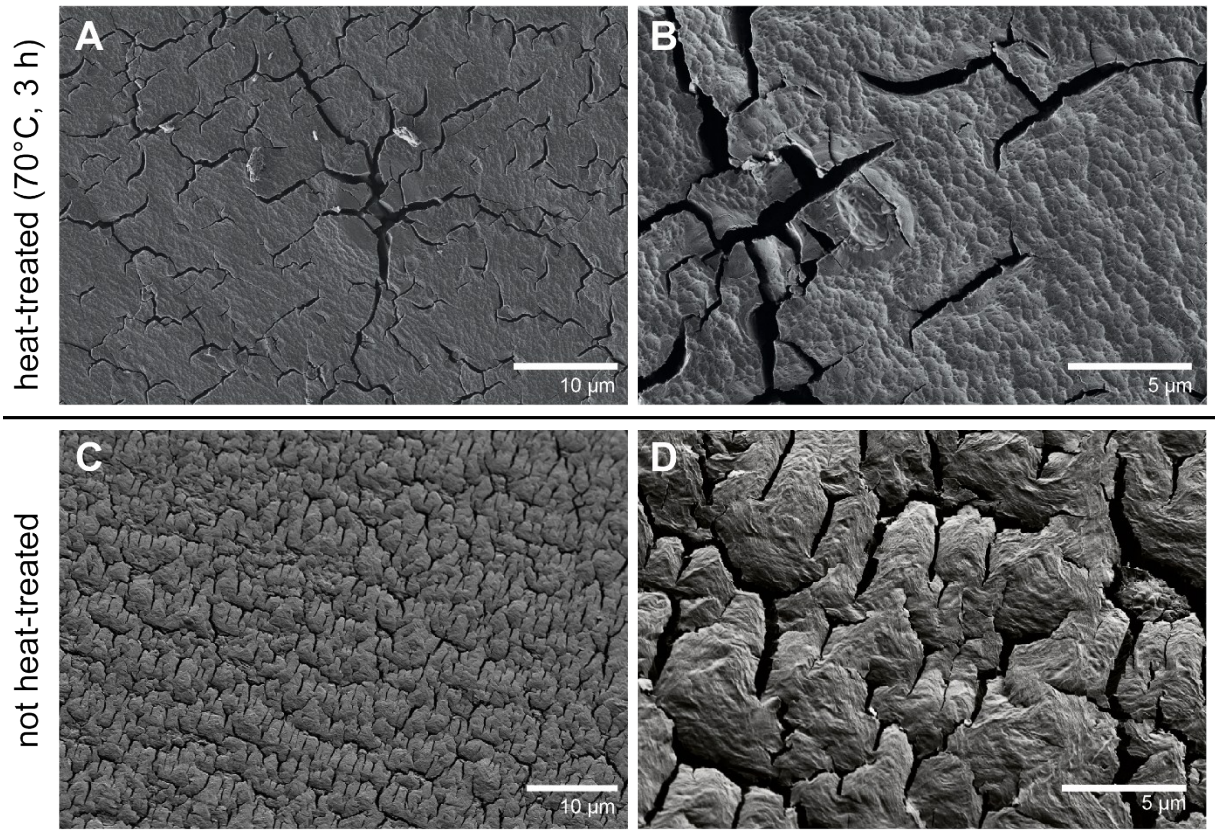

Fig. S4: (A, B) SEM images of a struvite crystal surface after heat-treatment at 70°C for 3 hours. **(C, D)** SEM images of a non-heat-treated struvite crystal surface. The non-heat treated crystal shows a much higher crack density compared to the heat treated one, possibly indicating that the decomposition process under high vacuum is more abrupt.

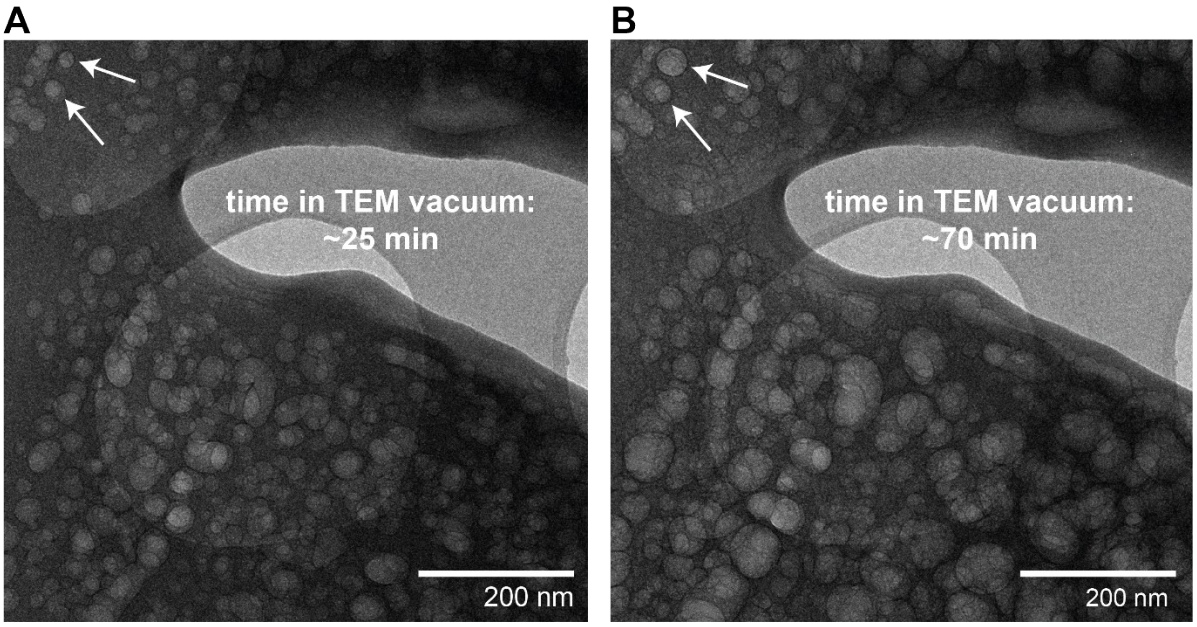

Fig. S5: Bright-Field TEM images obtained from a FIB section through a struvite crystal that was heat-treated at 90°C for ca. 3 hours. **(A)** Image taken after ca. 25 min in TEM vacuum showing abundant porosity. Two pores are indicated by white arrows. **(B)** After 70 min, significant widening of the pores had occurred suggesting ongoing decomposition due to the high vacuum conditions or electron beam sensitivity of the material.

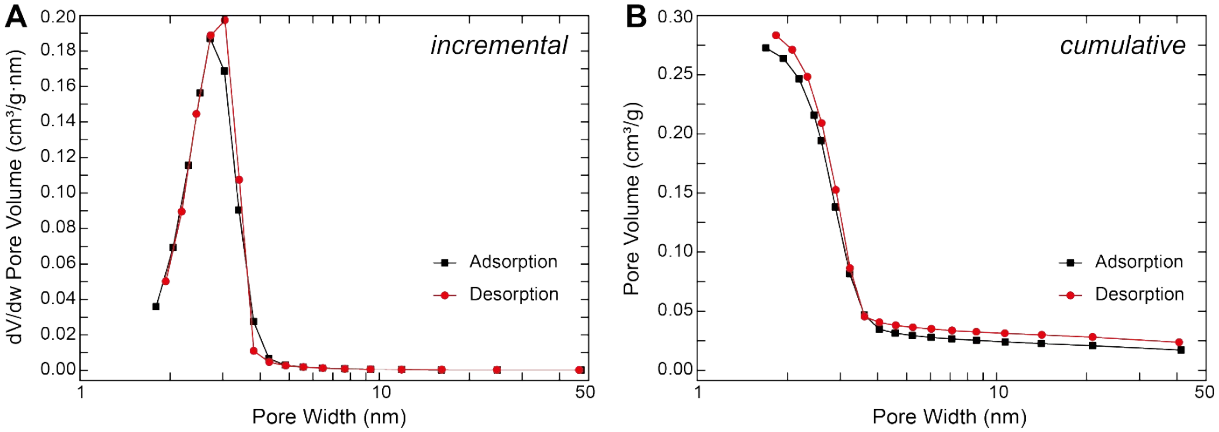

Fig. S6: BJH pore size distributions calculated from the adsorption (*red*) and desorption (*black*) branches of the sorption isotherm for a struvite sample heat-treated at 90°C for 80 min. **(A)** incremental and **(B)** cumulative pore size distributions.

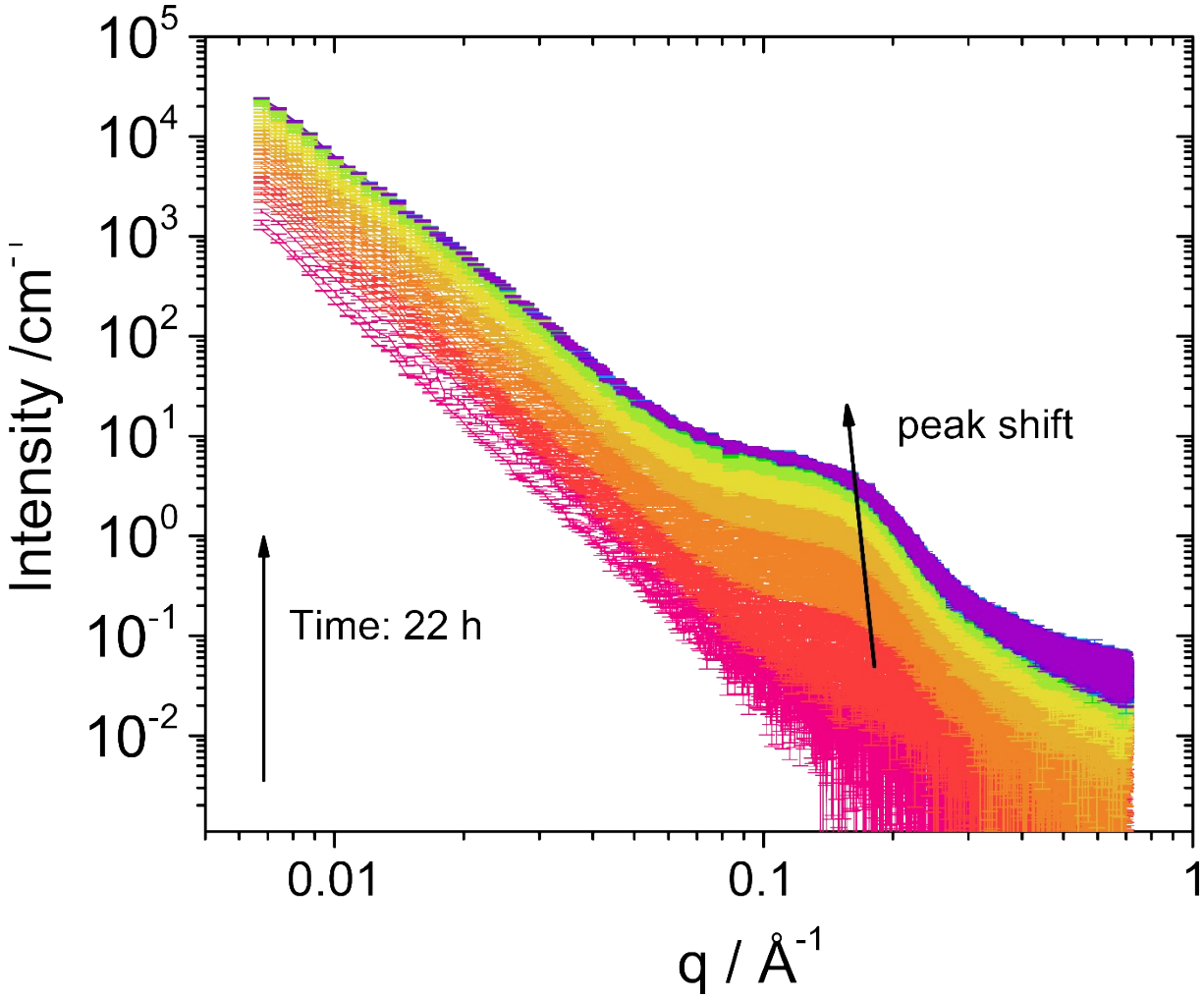

Fig. S7: Time-resolved SAXS patterns of struvite powders during vacuum (1 mbar) treatment at 40°C over the course of 22 hours. The time scale is encoded by a rainbow color palette (linear scale; pink = early times, purple = late times). With increasing time we observed that the overall scattering intensity gradually increases by at least an order of magnitude indicating an increase in surface area. After ~30 minutes, we observe a peak developing in the high-q part of the curves at q_{max} ~0.2 Å^{-1}. This scattering feature can be attributed to nano-sized pores forming within the bulk of the material. The SAXS patterns of the vacuum treated samples clearly differ from those of the thermally treated samples, since in the latter case we observed two distinct correlation peaks (the 1st maximum at ~0.1 Å^{-1} and the 2nd at ~0.21 Å^{-1}, see Fig. 5B in the main article). This suggests that the vacuum-treated samples have a more disordered (i.e., polydisperse) nanostructure. Over time, the data also show a slight peak shift towards lower q-values, i.e., from ~0.2 to ~0.15 Å^{-1}. This indicates an increase in the approximate pore diameter from ~3.2 to ~4.2 nm based on the relationship $d \approx 2\pi/q_{max}$.